J|A|C|S ARTICLES

Published on Web 03/01/2010

A Chiral Wedge Molecule Inhibits Telomerase Activity

Ken-ichi Shinohara,[†] Yuta Sannohe,[†] Shuji Kaieda,[†] Ken-ichi Tanaka,[‡] Hideji Osuga,[‡] Hidetoshi Tahara,[§] Yan Xu,[†,||] Takashi Kawase,[†] Toshikazu Bando,[†] and Hiroshi Sugiyama*[,†,⊥]

Department of Chemistry, Graduate School of Science, Kyoto University, Sakyo-ku Kyoto 606-8502, Japan, Department of Materials Science and Chemistry, Faculty of Systems Engineering, Wakayama University, 930 Sakaedani Wakayama 640-8510, Japan, Department of Cellular and Molecular Biology, Hiroshima University, Hiroshima 734-8553, Japan, Research Center for Advanced Science and Technology, The University of Tokyo, 4-6-1 Komaba Meguro-ku Tokyo 153-8904, Japan, and Institute for Integrated Cell-Material Sciences (iCeMS), Kyoto University, Sakyo-ku Kyoto 606-8501, Japan

Received October 19, 2009; E-mail: hs@kuchem.kyoto-u.ac.jp

Abstract: In addition to the Watson−Crick double helix, secondary DNA structures are thought to play important roles in a variety of biological processes. One important example is the G-quadruplex structure that is formed at the chromosome ends, which inhibits telomerase activity by blocking its access to telomeres. G-quadruplex structures represent a new class of molecular targets for DNA-interactive compounds that may be useful to target telomeres. Here, we reported the first example of enantioselective recognition of quadruplex DNA by a chiral cyclic helicene. We propose a new ligand-binding cleft between two telomeric human G-quadruplexes linked by a TTA linker. We found that the cyclic helicene M1 exhibited potent inhibitory activity against telomerase.

Introduction

Human telomeres, which are nucleoprotein complexes present at chromosome ends, consist of tandem arrays of TTAGGG repeats that can be elongated by adding single repeat units.[1−3] Telomerase is an important enzyme that is involved in telomere maintenance.[4,5] The enzyme is activated in 80−90% of human tumors and is low or undetectable in most normal somatic cells.[6] Thus, telomerase represents a target with good selectivity for tumorous over healthy tissues, and telomerase inhibition has been identified as a new approach to cancer therapy.[7−18] Folding of telomeric DNA into four-strand G-quadruplexes inhibits telomerase by locking the single-stranded telomeric substrate into an inactive conformation that is no longer recognized, nor elongated, by the enzyme.[19] Such quadruplexes are potential tumor-selective targets for chemotherapy.[19−22] Several quadruplex-specific ligands reportedly interact with quadruplexes and act as inhibitors of telomerase activity;[23−28] these include

[†] Graduate School of Science, Kyoto University.
[‡] Wakayama University.
[§] Hiroshima University.
[||] The University of Tokyo.
[⊥] iCeMS, Kyoto University.

(1) Blackburn, E. H. *Cell* **1994**, *77*, 621–623.
(2) Zakian, V. A. *Science* **1995**, *270*, 1601–1607.
(3) Greider, C. W. *Annu. Rev. Biochem.* **1996**, *65*, 337–365.
(4) McEachern, M. J.; Krauskopf, A.; Blackburn, E. H. *Annu. Rev. Genet.* **2000**, *34*, 331–358.
(5) Kim, N. W.; Piatyszek, M. A.; Prowse, K. R.; Harley, C. B.; West, M. D.; Ho, P. L.; Coviello, G. M.; Wright, W. E.; Weinrich, S. L.; Shay, J. W. *Science* **1994**, *266*, 2011–2015.
(6) Raymond, E.; Sun, D.; Chen, S. F.; Windle, B.; Von Hoff, D. D. *Curr. Opin. Biotechnol.* **1996**, *7*, 583–591.
(7) Hahn, W. C.; Stewart, S. A.; Brooks, M. W.; York, S. G.; Eaton, E.; Kurachi, A.; Beijersbergen, R. L.; Knoll, J. H.; Meyerson, M.; Weinberg, R. A. *Nat. Med.* **1999**, *5*, 1164–1170.
(8) Cech, T. R. *Angew. Chem., Int. Ed.* **2000**, *39*, 34–43.
(9) Shay, J. W.; Zou, Y.; Hiyama, E.; Wright, W. E. *Hum. Mol. Genet.* **2001**, *10*, 677–685.
(10) Rezler, E. M.; Bearss, D. J.; Hurley, L. H. *Curr. Opin. Pharmacol.* **2002**, *2*, 415–423.
(11) Mergny, J. L.; Riou, J. F.; Mailliet, P.; Teulade-Fichou, M. P.; Gilson, E. *Nucleic Acids Res.* **2002**, *30*, 839–865.
(12) Cairns, D.; Anderson, R. J.; Perry, P. J.; Jenkins, T. C. *Curr. Pharm. Des.* **2002**, *8*, 2491–2504.
(13) Huard, S.; Autexier, C. *Curr. Med. Chem. Anticancer Agents* **2002**, *2*, 577–587.
(14) Rezler, E. M.; Bearss, D. J.; Hurley, L. H. *Annu. Rev. Pharmacol. Toxicol.* **2003**, *43*, 359–379.
(15) Kelland, L. R. *Eur. J. Cancer* **2005**, *41*, 971–979.
(16) Shay, J. W.; Wright, W. E. *Nat. Rev. Drug Discovery* **2006**, *5*, 577–584.
(17) Pendino, F.; Tarkanyi, I.; Dudognon, C.; Hillion, J.; Lanotte, M.; Aradi, J.; Segal-Bendirdjian, E. *Curr. Cancer Drug Targets* **2006**, *6*, 147–180.
(18) Cian, A. D.; Lacroix, L.; Douarre, C.; Smaali, N. T.; Trentesaux, C.; Riou, J.; Mergny, J. L. *Biochimie* **2008**, *90*, 131–155.
(19) Zahler, A. M.; Williamson, J. R.; Cech, T. R.; Prescott, D. M. *Nature* **1991**, *350*, 718–720.
(20) Neidle, S.; Parkinson, G. N. *Nat. Rev. Drug Discovery* **2002**, *1*, 383–393.
(21) Chen, B.; Liang, J.; Tian, X.; Liu, X. *Biochemistry (Moscow)* **2007**, *73*, 853–861.
(22) Oganesian, L.; Bryan, T. M. *BioEssays* **2007**, *29*, 155–165.
(23) Read, M.; Harrison, R. J.; Romagnoli, B.; Tanious, F. A.; Gowan, S. H.; Reszka, A. P.; Wilson, W. D.; Kelland, L. R.; Neidle, S. *Proc. Natl. Acad. Sci. U.S.A.* **2001**, *98*, 4844–4849.
(24) Riou, J. F.; Guittat, L.; Mailliet, P.; Laoui, A.; Renou, E.; Petitgenet, O.; Megnin-Chanet, F.; Helene, C.; Mergny, J. L. *Proc. Natl. Acad. Sci. U.S.A.* **2002**, *99*, 2627–2677.
(25) Teulade-Fichou, M. P.; Carrasco, C.; Guittat, L.; Bailly, C.; Alberti, P.; Mergny, J. L.; David, A.; Lehn, J. M.; Wilson, W. D. *J. Am. Chem. Soc.* **2003**, *125*, 4732–4740.
(26) Jantos, K.; Rodriguez, R.; Ladame, S.; Shirude, P. S.; Balasubramanian, S. *J. Am. Chem. Soc.* **2006**, *128*, 13662–13663.

 10.1021/ja908897j

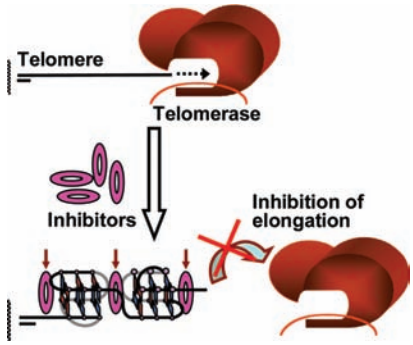

Figure 1. Schematic representation of telomerase inhibition by the G-quadruplex structure formed at the end of human chromosomes, which is stabilized by the binding of the ligand to the cleft pocket formed by the quadruplex dimer.

acridine derivatives, cationic porphyrin derivatives, and telomestatin.[29−33] Crystallographic, NMR, and computer modeling studies were performed to obtain detailed information on quadruplex structures and on the interaction of quadruplex DNA with, and stabilization by, small molecules.[34−38] Single quadruplex units (which are typically human telomeric sequences of 22 nt) were used as target structures in most of these previous studies. However, taking into account the length of the 3′-terminal single-stranded human telomeric DNA (100−200 bases),[39−41] a higher-order G-quadruplex structure would be formed in this region to inhibit telomerase activity (Figure 1a). Two groups proposed that two individual quadruplex structures could form a quadruplex dimer.[42,43] Recently, ours and two other groups demonstrated the formation of mixed parallel/antiparallel human telomeric G-quadruplexes with unique topology in K^+ solutions, suggesting the possibility of clustering of the 22 nt sequence units into higher-order packed structures.[44−49] However, it remains unclear how the ligands of G-quadruplex structures bind to telomeres in living cells (which contain a large amount of TTAGGG repeats) and lead to telomerase inhibition. We predict that the cleft pocket located between two telomeric human G-quadruplexes is formed in living cells when the G-quadruplexes are stabilized by the binding of the ligand (Figure 1a). Therefore, it would be important to use DNA molecules that are longer than 22 nt for the evaluation of G-quadruplex ligands. Recently, atomic force microscopy (AFM) observation of long telomeric DNA revealed the existence of consecutive G-quadruplex structures.[50] These superhelical structures may be suitable for ligand binding, which inhibits telomerase activity.

Here, we reported a cyclic helicene molecule that displayed chiral and steric selection during binding to quadruplex superhelical structures and exhibited potent inhibitory activity against telomerase. We reported previously that the simple helicene molecule (M)-A (Figure 2a) discriminates between B- and Z-DNA, binds to Z-DNA, and stabilizes Z-DNA conformation enantioselectively.[51] As the cleft pockets between G-quadruplex units should involve chiral-rich spaces and Z-DNA, here we investigated whether chiral helicene molecules had the ability to bind to the cleft pocket and stabilize G-quadruplex structures enantioselectively.

Results and Discussion

The newly targeted substrate ODN 1 (AGGG(TTAGGG)$_3$TTAGGG(TTAGGG)$_3$) used in this study consisted of a quadruplex dimer formed by two G-quadruplex repeats stacked 3′ to 5′ with a TTA linker. The ODN 2 substrate (AGGG(TTAGGG)$_3$(TTA)$_6$GGG(TTAGGG)$_3$), which contained six TTA repeats and in which the G-quadruplexes were divided into two separate units by the longer TTA repeated sequence, was used as a control. We first examined the binding of (P)-A and (M)-A to ODN 1 (Figure 2a). Both helicenes bound to ODN 1 but did not show enantioselectivity (Supporting Information Figure S1). We assumed that the dihedral angle of the helicene might contribute to the interaction; therefore, a series of chiral cyclic helicene molecules were prepared (Figure 2b). X-ray analysis indicated that the dihedral angle of the helical framework varied significantly from 22 to 59°, which suggests that the planarity of the helicenes decreased with the increasing length of the linker bridge.[52] The binding behavior of the helicenes to ODN 1 was examined using circular dichroism (CD) spectroscopy, which revealed an apparent 70% decrease in CD intensity during the binding of M1 to ODN 1, whereas no marked changes occurred during the binding of the other helicenes to ODN 1 (Figure 3a−c). To elucidate the molecular basis of the interaction of the helicene with the TTAGGG

(27) Brassart, B.; Gomez, D.; Cian, A. D.; Paterski, R.; Montagnac, A.; Qui, K. H.; Smaali, N. T.; Trentesaux, C.; Mergney, J. L.; Gueritte, F.; Riou, J. F. *Mol. Pharmacol.* **2007**, *72*, 631–640.
(28) Yu, H.; Wang, X.; Fu, M.; Ren, J.; Qu, X. *Nucleic Acids Res.* **2008**, *36*, 5695–5703.
(29) Koeppel, F.; Riou, J. F.; Laoui, A.; Mailliet, P.; Arimondo, P. B.; Labit, D.; Petitgenet, O.; Helene, C.; Mergny, J. L. *Nucleic Acids Res.* **2001**, *29*, 1087–1096.
(30) Han, H.; Langley, D. R.; Rangan, A.; Hurley, L. H. *J. Am. Chem. Soc.* **2001**, *123*, 8902–8913.
(31) Shin-ya, K.; Wierzba, K.; Matsuo, K.; Ohtani, T.; Yamada, Y.; Furihata, K.; Hayakawa, Y.; Seto, H. *J. Am. Chem. Soc.* **2001**, *123*, 1262–1263.
(32) Reed, J. E.; Arnal, A. A.; Neidle, S.; Vilar, R. *J. Am. Chem. Soc.* **2006**, *128*, 5992–5993.
(33) Baker, E. S.; Lee, J. T.; Sessler, J. L.; Bowers, M. T. *J. Am. Chem. Soc.* **2006**, *128*, 2641–2648.
(34) Clark, G. R.; Pytel, P. D.; Squire, C. J.; Neidle, S. *J. Am. Chem. Soc.* **2003**, *125*, 4066–4067.
(35) Gavathiotis, E.; Heald, R. A.; Stevens, M. F. G.; Searle, M. S. *J. Mol. Biol.* **2003**, *334*, 25–36.
(36) Parkinson, G. N.; Ghosh, R.; Neidle, S. *Biochemistry* **2007**, *46*, 2390–2397.
(37) Campbell, N. H.; Parkinson, G. N.; Reszka, Ap.; Neidle, S. *J. Am. Chem. Soc.* **2008**, *130*, 6722–6724.
(38) Parkinson, G. N.; Cuenca, F.; Neidle, S. *J. Mol. Biol.* **2008**, *381*, 1145–1156.
(39) Makarov, V. L.; Hirose, Y.; Langmore, J. P. *Cell* **1999**, *88*, 657–666.
(40) McElligott, R.; Wellinger, R. J. *EMBO J.* **1997**, *16*, 3705–3714.
(41) Wright, W. E.; Tesmer, V. M.; Huffman, K. E.; Levene, S. D.; Shay, J. W. *Genes Dev.* **1997**, *11*, 2801–2809.
(42) Haider, S.; Parkinson, G. N.; Neidle, S. *Biophys. J.* **2008**, *95*, 296–311.
(43) Petraccone, J.; Trent, J. O.; Chaires, J. B. *J. Am. Chem. Soc.* **2008**, *130*, 16530–16532.
(44) Xu, Y.; Noguchi, Y.; Sugiyama, H. *Bioorg. Med. Chem.* **2006**, *14*, 5584–5591.
(45) Ambrus, A.; Chen, D.; Dai, J.; Bialis, T.; Jones, R. A.; Yang, D. *Nucleic Acids Res.* **2006**, *34*, 2723–2735.
(46) Luu, K. N.; Phan, A. T.; Kuryavyi, V.; Lacroix, L.; Patel, D. J. *J. Am. Chem. Soc.* **2006**, *128*, 9963–9970.
(47) Matsugami, A.; Xu, Y.; Noguchi, Y.; Sugiyama, H.; Katahira, M. *FEBS J.* **2007**, *274*, 3545–3556.
(48) Phan, A. T.; Kuryavyi, V.; Luu, K. N.; Patel, D. J. *Nucleic Acids Res.* **2007**, *35*, 6517–6525.
(49) Dai, J.; Carver, M.; Punchihewa, C.; Jones, R. A.; Yang, D. *Nucleic Acids Res.* **2007**, *35*, 4927–4940.
(50) Xu, Y.; Ishizuka, T.; Kurabayashi, K.; Komiyama, M. *Angew. Chem., Int. Ed.* **2009**, *48*, 3281–3284.
(51) Xu, Y.; Zhang, Y. X.; Sugiyama, H.; Umano, T.; Osuga, H.; Tanaka, K. *J. Am. Chem. Soc.* **2004**, *126*, 6566–6567.
(52) Tanaka, K.; Osuga, H.; Kitahara, Y. *J. Org. Chem.* **2002**, *67*, 1795–1801.

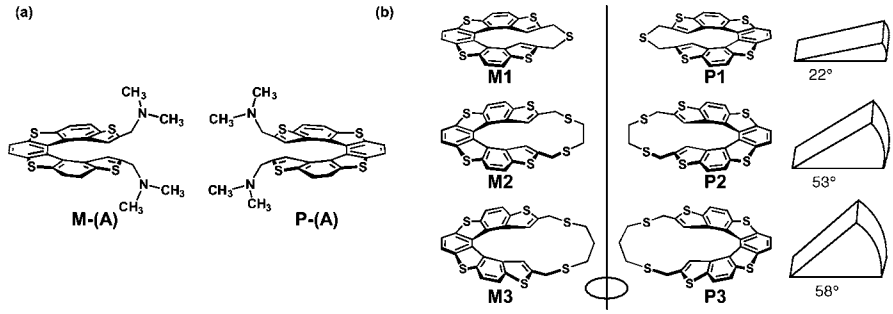

Figure 2. (a) Structures of the helicenes (M)-A and (P)-A, which bind enantioselectively to Z-DNA and B-DNA, respectively.[51] (b) Structures of the cyclic helicenes that were examined as higher-order G-quadruplex ligands. The dihedral angle of the helical frameworks increased from 22 to 58°.[52]

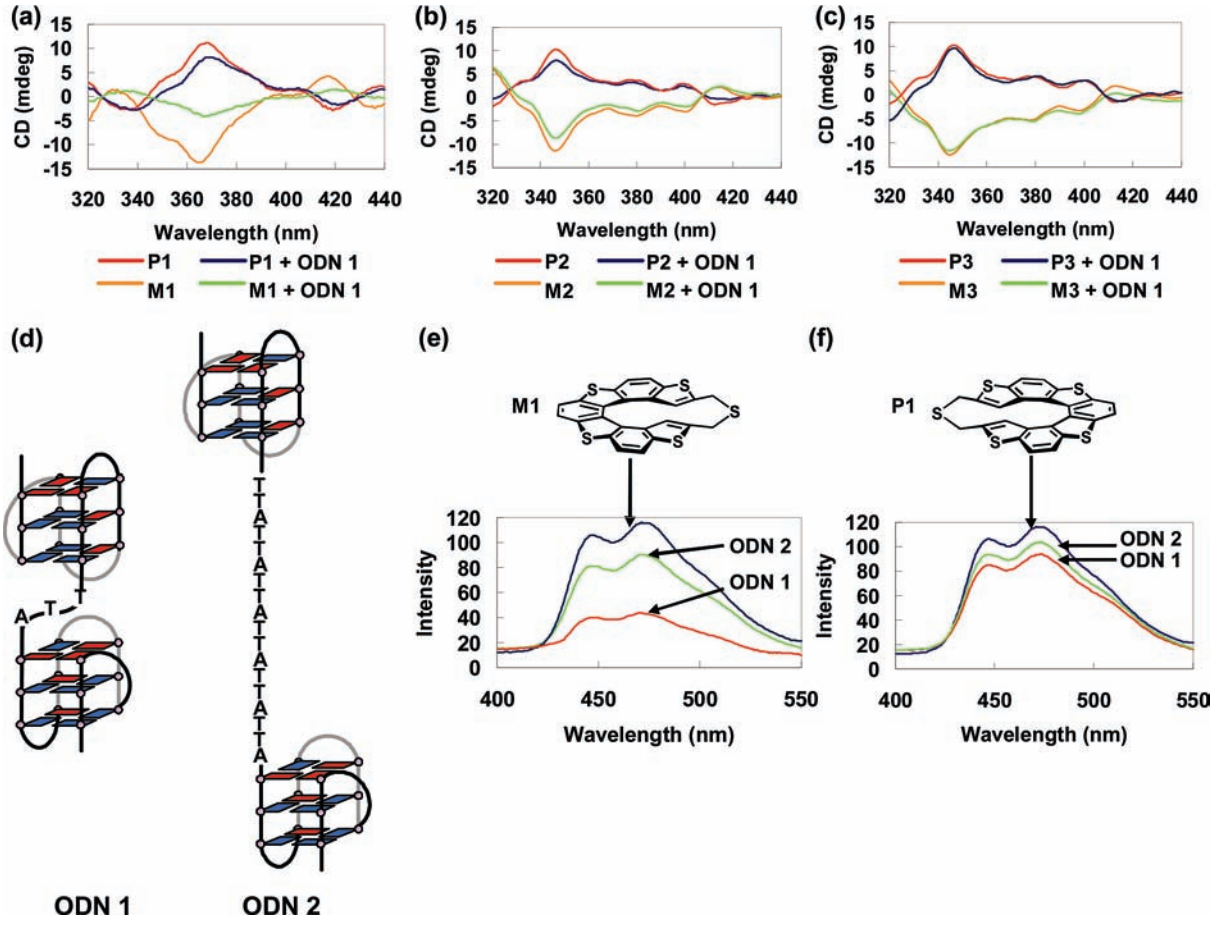

Figure 3. (a−c) CD spectra of the M1−M3 and P1−P3 helicenes (3 μM, 25 °C) in the presence or absence of ODN 1 (1.5 μM strand concentration) in 2 mM K-cacodylate buffer (pH 7.0) and in the presence of 150 mM KCl. (d) Targeted substrates used in the study; ODN 1 with a TTA linker formed a higher-order quadruplex dimer; ODN 2 with six TTA repeats was used as a control, as the longer bridge linker divided the G-quadruplexes into two separate units. (e,f) Fluorescence spectra (excitation at 330 nm) of (a) M1 and (b) P1 (1.0 μM, 25 °C) in 2 mM K-cacodylate buffer (pH 7.0), in the presence or absence of ODN 1 and ODN 2 in 100 mM KCl.

repeats, fluorescence measurements using ODN 2 were performed in parallel experiments. Strong quenching (80%) of the fluorescence of M1 was observed in the presence of ODN 1 compared with ODN 2 (Figure 3e). Conversely, P1 did not lead to a significant change in fluorescence after binding to ODN 1 or ODN 2 under the same conditions (Figure 3f). These results suggest that M1 binds preferentially to the dimer quadruplex ODN 1 in an enantioselective manner. The binding constants of helicene to DNA were examined using surface plasmon resonance (SPR) with biotinylated telomeric DNA. The observed SPR sensorgrams are shown in Figure 4. M1 exhibited a significant response curve at micromolar concentrations, whereas a response curve was not observed for P1, even at the concentration of 1 mM. The dissociation constants of M1 for ODN 1 and ODN 2 were estimated at 433(±13) and 475(±8) nM, respectively. Moreover, we investigated the binding of M1 to ODN 3, which contained four simple TTAGGG repeats (Supporting Information Figure S2). We observed an efficient reduction of fluorescence and a decrease in CD intensity in the presence of M1 and ODN 1, as shown in Figure 3, whereas there was no significant difference regarding the dissociation constants of M1 for ODN 1−3, as assessed using an SPR

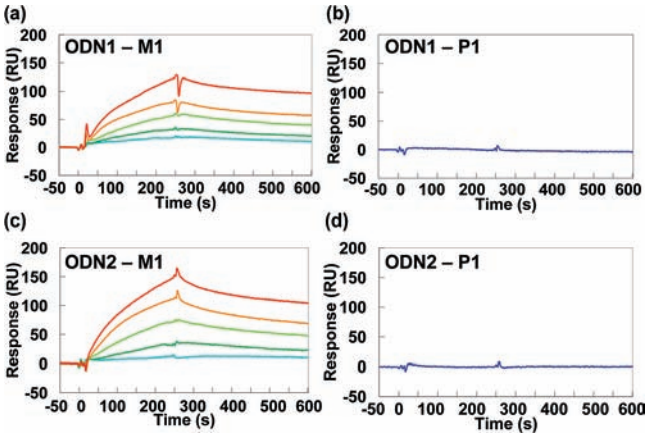

Figure 4. (a−d) SPR sensorgrams of the interaction of M1 and P1 with ODN 1 and ODN 2 in HEPES buffer (pH 7.4) in the presence of 200 mM KCl. The concentration of M1 ranged from 0.25 to 4 μM, and the concentration of P1 was 1 mM.

Table 1. Dissociation Constants of Helicene from DNA Determined Using the SPR Method (ODN 3 Contained Four Telomere Repeats)

	M1	P1
ODN 1	433 ± 13 nM	not determined
ODN 2	475 ± 8 nM	not determined
ODN 3	541 ± 11 nM	not determined

approach (Table 1). This discrepancy may be due to differences in the sensitivity of the methods or to the optical characteristic of the compounds. However, it is important to consider that P1 never bound to TTAGGG repeats. These results confirmed that M1 binds enantioselectively to quadruplex DNA.

Further analysis aimed at establishing the enantioselectivity of M1 and P1 was performed using the modified telomeric repeat amplification protocol (TRAP) assay—"stretch PCR".[53−55] In the presence of the M1 helicene, the assays revealed a dose-dependent inhibition of telomere ladder formation, which started at 0.2 μM and was completed at 0.5 μM; in contrast, no inhibition was observed in the presence of P1, even at 10 μM (Figure 5). In addition, the other helicenes described in Figure 2 did not inhibit telomerase activity (Supporting Information Figure S3). These results indicate clearly that M1 enantioselectively bound to single-stranded telomeric DNA and stabilized the G-quadruplex structure, which resulted in telomerase inhibition.

The preference of M1 for the G-quadruplex structure arose from the orientation of the left-handed helicene and shape complementarity with the dimer G-quadruplexes. To investigate the mechanism underlying the preferential binding of M1 to G-quadruplexes, a molecular model of the M1−DNA complex was estimated using energy minimization (Figure 6). We noted that a pocket was generated by the TTA linker, the two terminal G-tetrads of the dimer G-quadruplex,[43] and the TTA loops (Figure 6a). This suggests that M1 (with a shorter linker) was readily accommodated in the pocket, without any steric hindrance, whereas the helicenes M2, M3, P2, and P3, which

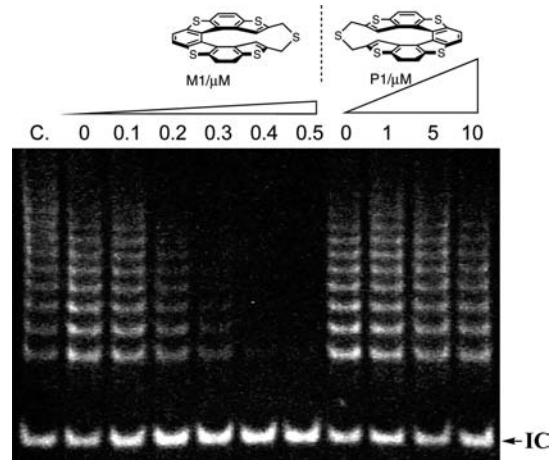

Figure 5. Inhibition of telomerase activity by M1 and P1 in vitro. Increasing concentrations of M1 (0−0.5 μM) or P1 (0−10 μM) solutions were added to the telomerase extract. The elongated products were amplified using PCR, which was followed by polyacrylamide gel electrophoresis. Lane C is a positive control, in which the buffer did not contain dimethyl formamide (DMF). The position of the internal standard is indicated as IC.

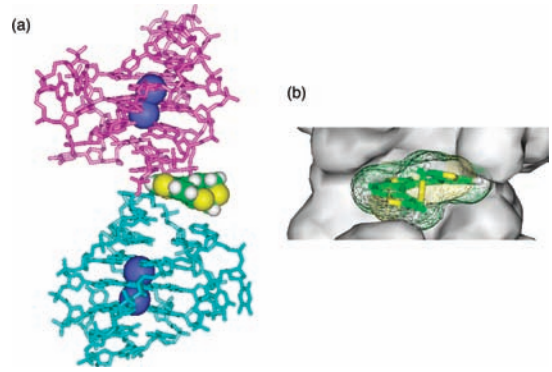

Figure 6. (a) Overall view of the energy-minimized structure of the complex formed by the G-quadruplex dimer[43] and M1. The dimer G-quadruplex structure is shown as a stick model (magenta and cyan), with M1 colored according to atom type. The K atoms in the central channel of the G-quartet are shown in blue. (b) Surface representation shows M1 (in stick representation) positioned in the cleft pocket.

contained longer linkers, introduced such steric clashes. Furthermore, the pocket itself had a special entrance, which suggests that the enantioselective binding of M1 may result from a preference by the cyclic helicene for snuggle binding to the cleft pocket, more so than P1 (Figure 6b). M1, which had a left-handed conformation, would be wedged tightly into this pocket (cleft), whereas P1, which had a right-handed conformation, would produce steric clashes that would prevent its burying deep within the pocket. The destruction of the pocket structure by the introduction of a longer linker (ODN 2) suggests that the cleft pocket played a role in the interaction of the helicene molecule with the G-quadruplex dimer.

Typically, the ligands of G-quadruplexes, such as telomestatin and TMPyP4, have flat structures. Our findings suggest that the dihedral angle of the helical frameworks should be considered as an important factor for the molecular design of G-quadruplex ligands in the future. The fact that M2 and M3 did not show any association to G-quadruplex DNA suggests that the dihedral angles of the cyclic molecules should be <50°. Although it remains unclear whether an angle of 22° is the most efficient, the critical angle should be close to this value. Thus, we

(53) Tatematsu, K.; Nakayama, J.; Danbara, M.; Shionoya, S.; Sato, H.; Omine, M.; Ishikawa, F. *Oncogene* **1996**, *13*, 2265–2274.
(54) Krupp, G.; Kuhne, K.; Tamm, S.; Klapper, W.; Heidorn, K.; Rott, A.; Parwaresch, R. *Nucleic Acids Res.* **1997**, *25*, 919–921.
(55) Gomez, D.; Mergny, J. L.; Riou, J. F. *Cancer Res.* **2002**, *62*, 3365–3368.

proposed a new ligand model for G-quadruplex-binding compounds based on insights collected from a chiral wedge molecule.

Conclusions

We found that a cyclic helicene with a short linker exhibited enantioselective binding to telomere repeats and enantioselective inhibition of telomerase. To the best of our knowledge, this is the first report demonstrating that a cyclic helicene has the properties of an enantioselective ligand that is capable of binding to telomeric G-quadruplexes. These results provide a proof-of-concept for small-molecule inhibitors of telomerase. The rational structure-based design of telomerase inhibitors necessitates a molecular understanding of the range of G-quadruplex topologies of serial G-quadruplex structures. Although we did not identify the actual models of binding of M1 to G-quadruplexes, our findings imply that the characteristics of ligands that stabilize G-quadruplexes can now be rationalized further.

Materials and Methods

Compounds and Oligonucleotides. Biotinylated DNA was purchased from Japan Bio Service Co. Ltd. The other unmodified DNA was purchased from Sigma Aldrich Japan. Those oligonucleotides were used without further purification. The synthesis of the helicene molecules was described previously.[52]

CD Measurements. CD spectra were measured using an AVIV Model 62 DS/202 CD spectrophotometer. CD spectra were recorded using a 1 cm path-length cell. Solutions for CD spectra were prepared as 0.4 mL samples of 3 μM of M and P helicenes, in the presence or absence of ODN 1 (1.5 mM strand concentration) in 2 mM K-cacodylate buffer (pH 7.0), in the presence of 150 mM KCl.

Fluorescence Measurements. Fluorescence spectra were measured using a JASCO FP-6300 spectrofluorometer. The samples were excited at 330 nm, and the fluorescence emission spectra were collected in the wavelength range of 350−550 nm. Solutions for fluorescence spectra were prepared as 0.1 mL samples at 1.0 μM of M1 and P1 in 2 mM K-cacodylate buffer (pH 7.0), in the presence or absence of ODN 1 and ODN 2 in 100 mM KCl.

SPR Assay. SPR experiments were performed using a BIACORE X instrument. The biotinylated ODN 1 (5′-biotin-TTTTTAGGG(TTAGGG)$_3$TTAGGG(GGGTTA)$_3$-3′), ODN 2 (5′-biotin-TTTTTAGGG(TTAGGG)$_3$(TTA)$_6$GGG(TTAGGG)$_3$-3′), and ODN 3 (5′-biotin-TTTTTAGGG(TTAGGG)$_3$-3′) oligos were immobilized on a streptavidin-coated sensor chip SA at a flow rate of 5 μL/min to obtain the desired immobilization levels. Experiments were performed using HBS-EP (10 mM HEPES, 150 mM NaCl, 3 mM EDTA, and 0.005% surfactant P20) buffer with 200 mM KCl and 0.1% DMF at 25 °C (pH 7.4). Sample solutions at various concentrations (0.25, 0.5, 1, 2, and 4 μM and 1 mM) were prepared in HBS-EP buffer with 200 mM KCl and 1% DMF and were injected at a flow rate of 5 μL/min. Data processing was performed by global fitting of the sensorgrams obtained experimentally to a model of 1:1 Langmuir binding using the BIAevaluation 4.1 software.

Molecular Modeling Studies. Minimizations were performed using the Discover software (MSI, San Diego, CA) with CFF forcefield parameters. The starting structure was built on the basis of the recent molecular dynamics simulation.[43] K cations were placed at the bifurcating position of the O−P−O angle, at a distance of 2.51 Å from the phosphorus atom. The resulting complex was soaked in a 10 Å layer of water. The whole system was minimized without any constraint to a stage where the rms was below 0.001 kcal/mol Å.

Cell Culture. Jurkat cells, which are human T-cell leukemia lymphoblast cells, were grown in RPMI1640 (Nacalai Tasque) supplemented with 10% fetal bovine serum (JRH Biosciences), 100 U/mL penicillin, and 100 μg/mL streptomycin at 37 °C in a 5% CO_2 atmosphere.

Telomerase Activity Assay−Stretch PCR. Telomerase activity in the presence of each helicene was evaluated using the stretch PCR[53] method on a TeloChaser system (Toyobo), according to the manufacturer's instructions, with minor modifications. Briefly, Jurkat cells were collected by centrifugation at 1000*g* for 5 min at 4 °C and washed twice with phosphate buffered saline (PBS; 140 mM NaCl, 2.7 mM KCl, 10 mM Na_2HPO_4, 1.8 mM KH_2PO_4, pH 7.3). To extract telomerase, cells were then treated with lysis solution at a concentration of 2.5×10^4 cells/μL. Forty microliters of the reaction mixtures, including 1.0 μL of the cell extract and 1.0 μL of helicene/*N*,*N*-DMF solution, was incubated at 37 °C for 45 min. Thirty cycles of PCR consisting of denaturing at 95 °C for 30 s, annealing at 68 °C for 30 s, and extension at 72 °C for 45 s were performed after the purification steps. The PCR products were electrophoresed in a 10% nondenaturing polyacrylamide gel in 0.5× buffer (45 mM Tris-HCl, 45 mM boric acid, 1 mM EDTA), followed by visualization by ethidium bromide staining.

Acknowledgment. This study was supported by a Grant-in-Aid for Priority Research from the Ministry of Education, Science, Sports, SORST, and CREST of the Japan Science and Technology (JST). The authors acknowledge the support by the Global COE Program "Integrated Materials Science". We also thank Dr. John O. Trent and Dr. Jonathan B. Chaires for coordinates of the Hybrid-12 model.

Supporting Information Available: Fluorescence spectra of (M)-A and (P), and SPR sensorgram of the interaction of (a) M1 and (b) P1 with ODN 3, and telomerase activities in the presence of the helicenes. This material is available free of charge via the Internet at http://pubs.acs.org.

JA908897J